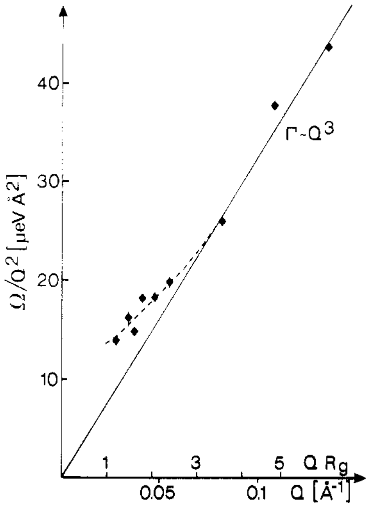

Figure 6. Reduced relaxation rates Ω/Q^2 obtained from the one-arm labeled star (PS120A) as a function of Q and v. The solid line represents the asymptotic Q^3 behavior due to internal Zimm modes. The dashed line indicates the slow crossover to translational diffusion.

pared to a linear polymer ($I \sim Q^{-1.5}$ instead of $I \sim Q^{-5/3}$). Perhaps this gives rise to effectively stiffer segments as $1/Q$ increases beyond a few bond lengths. The larger $1/Q$, the stiffer the mean segment, and the higher the characteristic frequency until $1/Q \gg R_g$. Then the center of mass diffusion dominates again.

In spite of the simple geometry of the multiarmed star branched polymer, the dynamics and structure of a finite size star polymer appear to be interesting and rich in physics. Through the advances in the modern synthetic chemistry, monodispersed star polymers with specific labeling by deuterium substitution can be produced. This allows the neutron scattering technique to probe not only the relation between structure and dynamics of the whole molecule but also any of the designated parts. We have learned that the characteristic minimum in the scaled line width of the collective relaxation of star polymers does not appear in the dynamics of a single-labeled arm in the star structure. Furthermore, the polystyrene star does not seem to obey the scaling behavior observed in the polyisoprene systems. Nevertheless, the static form factors of the polystyrene star and its labeled arms reflect the anomaly of the observed dynamics. A more fundamental theoretical approach to these observations should prove useful for the understanding of not only the star polymers but also other branched system, including polymer networks.

Registry No. Neutron, 12586-31-1; polystyrene, 9003-53-6.

References and Notes

(1) For an overview, see, e.g.: Burchard, W. In *Advances in Polymer Science*; Cantow, H. J., et al., Eds.; Springer Verlag: Berlin, Heidelberg, New York, 1983; Vol. 48.
(2) Daoud, M.; Cotton, J. P. *J. Phys.* (*Les Ulis, Fr.*) **1982**, *43*, 531.
(3) Huber, K.; Burchard, W.; Fetters, L. J. *Macromolecules* **1984**, *17*, 541.
(4) Dozier, W. D.; Huang, J. S.; Fetters, L. J., unpublished results.
(5) Richter, D.; Stühn, B.; Ewen, B.; Nerger, D. *Phys. Rev. Lett.* **1987**, *58*, 2462.
(6) Khasat, N.; Pennisi, R. W.; Hadjichristidis, N.; Fetters, L. J. *Macromolecules*, in press.
(7) Grest, G. S.; Kremer, K.; Witten, T. A. *Macromolecules* **1987**, *20*, 1376.
(8) Stockmayer, W. H.; Fixman, M. *Ann. N. Y. Acad. Sci.* **1952**, *57*, 334.
(9) de Gennes, P.-G. *Physica* (*Utrecht*) **1959**, *25*, 825.
(10) Khasat, N.; Pennisi, R. W.; Hadjichristidis, N.; Fetters, L. J. *Macromolecules* **1988**, *21*, 1100.
(11) Benoit, H. *J. Polymer Sci.* **1953**, *11*, 507.
(12) Huber, K.; Bantle, S.; Burchard, W.; Fetters, L. J. *Macromolecules* **1986**, *19*, 1404.
(13) Huber, K.; Burchard, W.; Bantle, S.; Fetters, L. J. *Polymer* **1987**, *28*, 1900, 1997.
(14) Mezei, F. In *Lecture Notes in Physics*; Mezei, F., Ed.; Springer-Verlag: Berlin, Heidelberg, New York, 1980; Vol. 128.
(15) Dubois-Violette, E.; de Gennes, P.-G. *Physics* (*Long Island City, N. Y.*) **1967**, *3*, 181.
(16) Witten, T. A.; Pincus, P. A.; Cates, M. E. *Europhys. Lett.* **1986**, *2*, 137.
(17) Nicholson, L. K.; Higgins, J. S.; Hayter, J. B. *Macromolecules* **1981**, *14*, 836.
(18) Mas, J. W.; Hadjichristidis, N.; Fetters, L. J. *Macromolecules* **1985**, *18*, 2330.
(19) Hadjichristidis, N.; Xu, C.; Fetters, L. J.; Roovers, J. *J. Polym. Sci., Polym. Phys. Ed.* **1982**, *20*, 743.
(20) Nicholson, L. K.; Higgins, J. S.; Hayter, J. B. *Proceedings of the 27th International Symposium on Macromolecules*; Strasbourg, July 6–9, 1981.

Chain Configurations in Semicrystalline Interphases: Chain Stiffness

J. A. Marqusee

Polymers Division, National Bureau of Standards, Gaithersburg, Maryland 20899, and Institute for Defense Analyses, 1801 N. Beauregard Street, Alexandria, Virginia 22311.
Received February 24, 1988; Revised Manuscript Received June 27, 1988

ABSTRACT: A previously presented mean-field lattice theory (*Macromolecules* **1986**, *19*, 2420) is extended to treat chain stiffness. The effect of bending energy on the configurational properties of chains at semicrystalline interfaces is analyzed. The width of the interfacial region and the degree of adjacent reentry are presented as a function of chain stiffness. A comparison with the case of chains bounded by a hard wall is given.

Introduction

The configurations of long-chain molecules at the crystal/amorphous interface in semicrystalline polymeric materials has been actively debated for a number of years.[1-3] A melt of long-chain molecules when cooled forms a series of lamellar crystals which are separated by amorphous regions. The chains can be many times longer than the width of these lamellae and thus they may possibly traverse the crystal and amorphous regions many times.

A large number of the chains which exit the crystal must reenter it so as to avoid an anomolously high density in

0024-9297/89/2222-0472$01.50/0

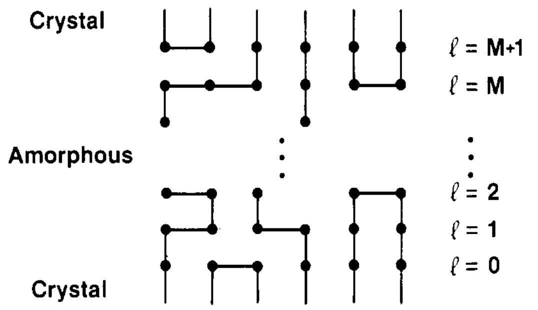

Figure 1. Schematic cross-sectional view of the amorphous region in a lamellar semicrystalline polymer.

the amorphous region.[1,4] An issue which has led to heated discussions[2] is whether chains reenter the crystal at sites adjacent to where they exit or whether they reenter more randomly. Related to this issue is the question of how wide the interfacial region is. Models which treat the entire amorphous region as bulk polymer[5-7] assume an infinitely sharp interface. A number of lattice models have been introduced which predict a finite interfacial region where there is a gradual transition from the crystal to the amorphous region.[8-10]

In a recent paper,[10] hereafter referred to as paper I, we generalized an approach developed by Helfand[11,12] and applied it to the semicrystalline interphase. This approach allows one to take into consideration the constraints imposed by the interface on the chain configurations and systematically treat correlations among bonds along the chain. In paper I we analyzed the case of freely flexible chains at the semicrystalline interface. In this paper we continue that analysis by including the possibility of an internal energy in the form a simple bending energy. A mean-field treatment is given for the chain configurations at an interface when chain stiffness must be considered. Results are presented for the width and degree of adjacent reentry for the semicrystalline polymer interface as a function of chain stiffness. For comparison, the case of a polymer melt against a hard wall is also considered.

We model the amorphous region of the polymer with a cubic lattice. The crystalline region is assumed to be devoid of defects and is accounted for by suitable boundary conditions on the chain configurations. The lattice is divided into a set of layers, enumerated by the index l, parallel to the crystal interface. The crystal terminates at $l = 0$ and begins again at $l = M + 1$ (see Figure 1). This represents an amorphous region bounded by a crystalline polymer.

The polymer chains are modeled as linearly connected walks on the cubic lattice. We characterize a particular set of configurations by the sequence $R = (r, ..., r_k, ...)$ where r_k is the location of the lattice site which contains the kth segment. All lattice sites are singly occupied by a polymer segment. Details of the model may be found in paper I.

The chain configurations are obtained by minimizing the free energy. Thus the results presented here assume the configurations in the amorphous region are determined by equilibrium considerations rather than kinetic limitations.

Configurational Free Energy

The configurational entropy of chains in the interphase differs considerably from that in the bulk even in the absence of chain stiffness. In paper I, following Helfand,[10,11] we derived the configurational entropy in terms of local chain statistics in a mean-field approximation. Here the configurational entropy is treated at the level of the two-segment approximation, so as to systematically include the effects of bending energy.

The configurational entropy is given by

$$S = k_B \sum_R P_0(R) \ln P_0(R) \tag{1}$$

plus additive constants which are independent of the local chain statistics and thus irrelevant for our purposes. $P_0(R)$ is the mean-field probability of a configuration R and is not explicitly subject to excluded-volume restrictions.

The chain probability can be written as the product of conditional probabilities

$$P_0(R) = \prod_k p(r_{k+1}|r_k,r_{k-1}) \tag{2}$$

where $p(r_{k+1}|r_k,r_{k-1})$ is the probability that the $k + 1$ segment is at r_{k+1} given that the k and $k - 1$ segments are at r_k and r_{k-1}, respectively. The conditional probability's dependence on the location of the previous segments has been truncated to the previous two segments. This is the simplest level at which one may treat the chain statistics and include chain stiffness. Substituting eq 2 into eq 1 yields

$$S = k_B \sum_k \sum_{r_{k+1},r_k,r_{k-1}} p(r_{k+1},r_k,r_{k-1}) \ln p(r_{k+1}|r_k,r_{k-1}) \tag{3}$$

where end effects have been neglected. The three-segment joint probability is a product of three factors

$$p(r_{k+1},r_k,r_{k-1}) = p(r_{k+1}|r_k,r_{k-1})\, p(r_k|r_{k-1})\, p(r_{k-1}) \tag{4}$$

where $p(r_k|r_{k-1})$ is the one-segment conditional probability and $p(r_{k-1})$ is the single-segment probability. In the long-chain limit all segments along the chain are equivalent. In this limit the single-segment distribution has no spatial dependence and all sets of segments $k + 1$, k, $k - 1$ are equivalent. Under these assumptions the entropy may be expressed as

$$S = -k_B \sum_{r_{k+1},r_k,r_{k-1}} p(r_{k+1}|r_k,r_{k-1})\, p(r_k|r_{k-1}) \ln p(r_{k+1}|r_k,r_{k-1}) \tag{5}$$

Details of the above derivation may be found in paper I.

The configurational energy is solely due to bending energy. In general we may write the thermodynamic energy as

$$E = \sum_R E(R)\, P_0(R) \tag{6}$$

in a mean-field approximation. We consider here only the simplest bending energy which depends on three consecutive segments (or two bonds)

$$E = \sum_k \sum_{r_{k+1},r_k,r_{k-1}} p(r_{k+1},r_k,r_{k-1})\, E(r_{k+1},r_k,r_{k-1}) \tag{7}$$

where we have again neglected end effects. Decomposing the three-segment joint probability as in eq 4 and using the invariance along the chain reduce eq 7 to

$$E = \sum_{r_{k+1},r_k,r_{k-1}} p(r_{k+1}|r_k,r_{k-1})\, p(r_k|r_{k-1})\, E(r_{k+1},r_k,r_{k-1}) \tag{8}$$

The configurational free energy is simply given by

$$F = E - TS \tag{9}$$

where E and S are given by eq 8 and eq 5, respectively. To determine the local chain statistics and to analyze the effect of bending energy, we minimize the free energy subject to the appropriate boundary conditions and constraints on the conditional probabilities.

Interphase

In the case of the semicrystalline polymer and other interphases, we assume the conditional probabilities depend solely on the distance from the interface and are the same for all sites in a given layer. Consider the kth segment to be in the lth layer. The one-segment conditional probability for steps to neighboring sites is

$$\begin{aligned} p(r_{k+1}|r_k) &= p_l(+) \qquad r_{k+1} \text{ in } l+1 \\ p(r_{k+1}|r_k) &= p_l(0) \qquad r_{k+1} \text{ in } l \\ p(r_{k+1}|r_k) &= p_l(-) \qquad r_{k+1} \text{ in } l-1 \end{aligned} \tag{10}$$

as in paper I. For the two-segment conditionals we slightly generalize the previous notation. Previously we defined nine two-segment conditional probabilities for three segments in neighboring sites

$$p(r_{k+1},r_k,r_{k-1}) = \left[\begin{matrix} p_l(+|+) & p_l(+|0) & p_l(+|-) \\ p_l(0|+) & p_l(0|0) & p_l(0|-) \\ p_l(-|+) & p_l(-|0) & p_l(-|-) \end{matrix}\right] \tag{11}$$

where $p(\alpha|\beta)$ is the probability that segment $k+1$ is in layer $l+\alpha$ given that segment k is in layer l and segment $k-1$ is in layer $l+\beta$. α and β represent either +, 0, or −. To properly include bending energies, we must differentiate between two types of steps within a given layer. $p_l(0|0)$, the conditional probability for steps that have all three segments in layer l, is replaced by two conditional probabilities. They are, $p_l^{(s)}(0|0)$ for steps in which all three segments are linear and $p_l^{(b)}(0|0)$ for steps which have a 90° bend. The third possibility of an immediate reversal is not allowed. To completely eliminate this unphysical configuration we set

$$p_l(+|+) = p_l(-|-) = 0 \tag{12}$$

The free energy can now be expressed as a sum over layers. The sum over r_k is replaced by $N_0\sum_l$ where N_0 is the number of sites in a layer. The sums over r_{k+1} and r_{k-1} contribute only for neighboring sites. Substituting the above definitions for the conditional probabilities into eq 5 yields

$$\begin{aligned} S = -k_B N_0 \sum_l \{&4p_l(+|0)\, p_l(0) \ln p_l(+|0) + \\ &p_l(+|-)\, p_{l-1}(+) \ln p_l(+|-) + 4p_l(0|+)\, p_{l+1}(-) \ln p_l(0|+) + \\ &8p_l^{(b)}(0|0)\, p_l(0) \ln p_l^{(b)}(0|0) + \\ &4p_l(0|-)\, p_{l-1}(+) \ln p_l(0|-) + p_l(-|+)\, p_{l+1}(-) \ln p_l(-|+) + \\ &4p_l(-|0)\, p_l(0) \ln p_l(-|0) + 4p_l^{(s)}(0|0)\, p_l(0) \ln p_l^{(s)}(0|0)\} \end{aligned} \tag{13}$$

where the numerical factors arise from the four possible directions in a given layer in a cubic lattice.

The energy can be similarly reduced. We take the configuration of three collinear segments as the zero of energy and assign an energy ϵ_b to bent configurations. Under this convention the energy is

$$\begin{aligned} E = N_0\epsilon_b \sum \{&4p_l(+|0)\, p_l(0) + 4p_l(0|+)\, p_{l+1}(-) + \\ &8p_l^{(b)}(0|0)\, p_l(0) + 4p_l(0|-)\, p_{l-1}(+) + 4p_l(-|0)\, p_l(0)\} \end{aligned} \tag{14}$$

The conditional probabilities are not free to take on all values. There are constraints due to the boundary conditions imposed by the interface plus two additional types of constraints. The first is that the conditional probabilities must be normalized

$$\sum_{r_{k+1}} p(r_{k+1}|r_k) = 1 \tag{15}$$

and

$$\sum_{r_{k+1}} p(r_{k+1}|r_k,r_{k-1}) = 1 \tag{16}$$

In the case of an interphase and a cubic lattice these reduce to

$$p_l(+) + 4p_l(0) + p_l(-) = 1 \tag{17}$$

and

$$\begin{aligned} 4p_l(0|+) + p_l(-|+) &= 1 \\ p_l(+|0) + 2p_l^{(b)}(0|0) + p_l^{(s)}(0|0) + p_l(-|0) &= 1 \\ p_l(+|-) + 4p_l(0|-) &= 1 \end{aligned} \tag{18}$$

The second constraint is due to the symmetry of the polymer configuration with respect to its two ends. The probability of a configuration in one direction must be equal to the probability for the same configuration taken in the opposite direction along the chain. This symmetry requirement constrains the one-segment conditional probabilities

$$p_l(+) = p_{l+1}(-) \tag{19}$$

and the two-segment conditional probabilities

$$\begin{aligned} p_l(+|0)\, p_l(0) &= p_l(0|+)\, p_{l+1}(-) \\ p_l(+|-)\, p_{l-1}(+) &= p_l(-|+)\, p_{l+1}(-) \\ p_l(0|-)\, p_{l-1}(+) &= p_l(-|0)\, p_l(0) \end{aligned} \tag{20}$$

as shown previously. These constraints ensure that in the mean the lattice is uniformly and completely filled by chain segments.[10]

In a bulk system there are no boundary constraints on the probabilities and they are translationally invariant. Minimizing the free energy subject to the normalization and symmetry constraints simply yields the nonreversing random walk values

$$p(r_{k+1}|r_k,r_{k-1}) = 1/5 \qquad p(r_{k+1}|r_k) = 1/6 \tag{21}$$

in the absence of any bending energies. The bending energy alters the two-segment conditional probabilities. One obtains the standard Boltzmann form

$$p(r_{k+1}|r_k,r_{k-1}) = \frac{e^{-\epsilon_b/k_BT}}{1 + 4e^{-\epsilon_b/k_BT}} \tag{22}$$

for a bent configuration and

$$p(r_{k+1}|r_k,r_{k-1}) = \frac{1}{1 + 4e^{-\epsilon_b/k_BT}} \tag{23}$$

for a straight configuration.

The presence of the crystal fixes the probabilities at the boundaries. To determine the chain statistics in the interphase, the free energy must be minimized subject to the above constraints and the boundary conditions

$$P_0(-) = 1/2 \qquad P_0(+|0) = 0 \qquad P_0(-|0) = 1 \tag{24}$$

and

$$\begin{aligned} P_{M+2}(-) = 1/2 \qquad P_{M+1}(-|0) = 0 \\ P_{M+1}(+|0) = 1 \end{aligned} \tag{25}$$

These boundary conditions break the translational invariance and couple the conditional probabilities so as to invalidate a simple Boltzmann relation between all bent and straight configurations.

The relative weight of the two-segment conditional probabilities for the bent and straight configurations when all three segments are in the same layer does obey a simple Boltzmann relation. Since the three segments are all the same distance from the interface, the perturbation due to the interface is equivalent for the two configurations. Minimization of the free energy with respect to $p_l^{(b)}(0|0)$ subject to the normalization constraint, eq 18, yields

$$p_l^{(b)}(0|0) = e^{-\epsilon_b/k_BT} p_l^{(s)}(0|0) \tag{26}$$

Table I
Conditional Probabilities and Order Parameter $\epsilon_b = 0$

l	$p_l(-)$	$p_l(+\|0)$	$p_l(-\|0)$	S_l
0	0.5	0	1	0.451
1	0.134	0.207	0.155	−0.045
2	0.170	0.199	0.205	0.005
3	0.166	0.200	0.200	−0.001
4	0.167	0.200	0.200	0

Table II
Conditional Probabilities and Order Parameter $\epsilon_b = k_BT$

l	$p_l(-)$	$p_l(+\|0)$	$p_l(-\|0)$	S_l
0	0.5	0	1	0.608
1	0.239	0.138	0.240	0.127
2	0.179	0.147	0.163	0.022
3	0.169	0.149	0.151	0.004
4	0.167	0.149	0.149	0.001

Table III
Conditional Probabilities and Order Parameter $\epsilon_b = 2k_bT$

l	$p_l(-)$	$p_l(+\|0)$	$p_l(-\|0)$	S_l
0	0.5	0	1	0.772
1	0.352	0.072	0.305	0.419
2	0.261	0.082	0.172	0.213
3	0.214	0.085	0.126	0.107
4	0.190	0.087	0.106	0.053
5	0.170	0.088	0.097	0.026
6	0.175	0.088	0.092	0.013
7	0.170	0.088	0.088	0.007

as in the bulk.

Similar simple relations do not hold for the other conditional probabilities. Minimization of the free energy with respect to the other conditional probabilities subject to the constraint equations yields a set of coupled difference equations which must be solved numerically for the one- and two-segment conditional probabilities.

Results

The resulting difference equations obtained by minimizing the free energy are solved numerically as a set of simultaneous equations for a fixed number of amorphous layers M and a given bending energy ϵ_b/k_BT. We have obtained the conditional probabilities for bending energies ranging from freely flexible chains with $\epsilon_b = 0$ to fairly stiff chains with $\epsilon_b = 2k_BT$.

The conditional probabilities are relatively insensitive to the width or the amorphous zone, M. For freely flexible chains the chain statistics approximately decay to their amorphous values by the fourth layer, given that the crystal terminates at the zeroth layer. When one considers amorphous zones with widths more than twice this distance the conditional probabilities are effectively independent of M. For the stiffest chains we consider, $\epsilon_b = 2k_BT$, the chain statistics do not reach their amorphous values until the 11th layer. In this case one must consider much larger amorphous zones to eliminate the dependence on M. All the results presented here are for widths sufficiently large so as to eliminate the dependence on M. For narrower amorphous zones the conditional probabilities are only altered by a few percent for layers before the midpoint of the zone.

In Tables I, II, and III are listed the conditional probabilities for the interphase. The results are for chains with bending energies 0, k_BT, and $2k_BT$ respectively. The other conditional probabilities may be constructed by using the appropriate constraint equations. The one-segment conditionals should be compared to the amorphous value of $^1/_6$. The two-segment conditional probabilities for bent configurations should be compared to the amorphous values of $^1/_5$ for $\epsilon_b = 0$ and 0.149 for $\epsilon_b = kT$ and 0.088 for $\epsilon_b = 2k_BT$.

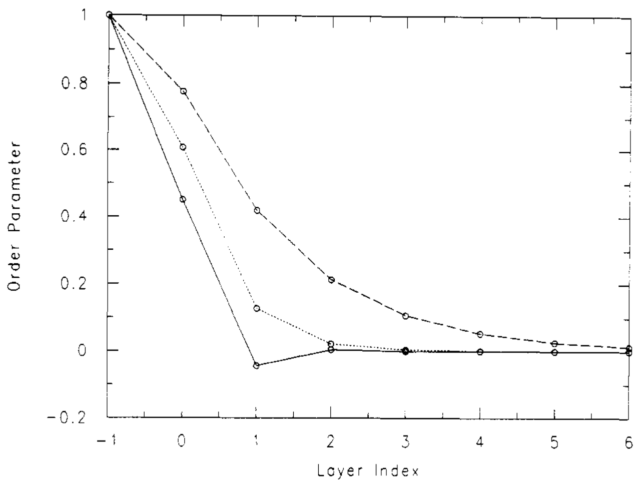

Figure 2. Bond orientational order parameters as a function of distance from the crystal. The results are for three bending energies: $\epsilon_b = 0$ (—), $\epsilon_b = k_BT$ (···), and $\epsilon_b = 2k_BT$ (- - -).

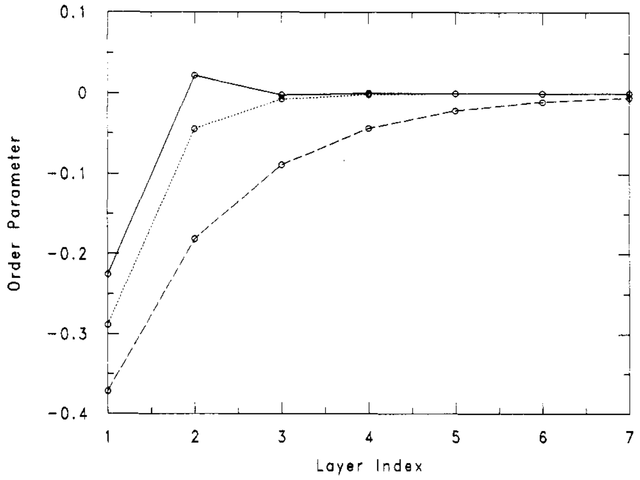

Figure 3. Bond orientational order parameters as a function of distance from a hard wall. The results are for three bending energies: $\epsilon_b = 0$ (—), $\epsilon_b = k_BT$ (···), and $\epsilon_b = 2k_BT$ (- - -).

Also listed are the orientational order parameters. The order parameter in each layer is

$$S_l = 1 - \tfrac{3}{2}\langle \sin^2 \theta_l \rangle \qquad (27)$$

where θ_l is the angle between a bond and the normal to the crystal in the lth layer. This can be expressed as

$$S_l = 1 - 6p_l(0) \qquad (28)$$

for a cubic lattice.

As the bending energy increases the width of the interphase increases. This can clearly be seen in a plot of the orientational order parameter versus layer index, Figure 2. For freely flexible chains the perfect order of the crystal dissipates very rapidly, slightly overshooting random orientations at layer 1 where the bonds have a small preference to orient parallel to the crystal interface. Even a small bending energy will dampen out this overshoot to yield a monotonic decay to the amorphous state. As the bending energy increases the decay of the orientational order slows and the crystal presence is felt many layers into the amorphous region.

The magnitude of the orientational order and its direction are specifically due to the boundary conditions imposed by the crystal. The width of the interphase and its dependence on chain stiffness is a general feature of

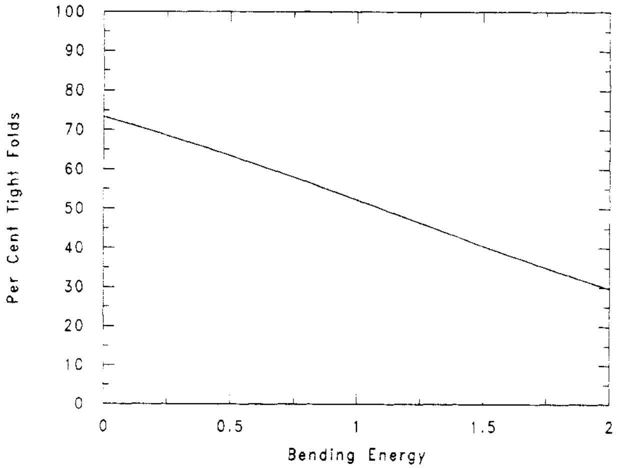

Figure 4. Percent of chains involved in tight folds at the 0th layer versus the bending energy in units to k_BT.

interphases. For comparison, the orientational order parameter for long chains bounded by a hard wall is shown in Figure 3. The wall is situated at layer $l = 0$ and imposes the boundary conditions on the chain statistics

$$P_1(-) = 0 \qquad P_1(-|0) = 0 \qquad P_1(-|+) = 0 \tag{29}$$

Minimizing the free energy subject to these boundary conditions yields the results shown in Figure 3. Contrary to the semicrystalline case, the wall induces a parallel orientation of the bonds. But the changes due to increased stiffness are very similar and the widths of the interphase for these very different boundary conditions are also quite similar.

The effect of a wall on the configurations of a freely flexible chain in a melt has been previously treated by using a lattice description by Weber and Helfand[13] as well as Yoon and Flory.[14] Our approach is a generalization of Helfand's, and thus as expected, the predictions for the zero bending energy case are very similar. Yoon and Flory predict a smaller parallel orientation of the chains to the wall in the first layer for zero bending energy. Their predictions are in error due to an improper counting of chain configurations.[10]

More detailed properties of the interphase can be constructed by using the conditional probabilities listed in Tables I, II, and III. Increased chain stiffness leads to a substantial decrease in the number of chains involved in tight folds at the 0th layer. A plot of the percent of chains involved in tight folds in the 0th layer versus the bending energy is given in Figure 4. The percent of 0th-order tight folds decays essentially linearly from 73.3% at $\epsilon_b = 0$ to 52.2% at $\epsilon_b = k_BT$ and finally 29.7% at $\epsilon_b = 2k_BT$. While the increased bending energy decreases the number of immediate reversals, it increases the number of tight folds that occur in the next layer, $l = 1$. They increase from 3.3% for $\epsilon_b = 0$ to 6.7% for $\epsilon_b = k_BT$ and 7.3% for $\epsilon_b = 2k_BT$. The increased stiffness extends the region of the interphase by essentially delaying the occurrence of tight folds.

The previous lattice models for Flory, Yoon, and Dill[9] (FYD) and Mansfield[8] have also investigated the effects of chain stiffness. It is difficult to make a direct comparison with the work of FYD due to the large differences in their predictions for freely flexible chains and those presented here and in paper I. As previously pointed out,[10] FYD incorrectly approximated the partition function for freely flexible chains. This led to their erroneous predictions for freely flexible chains as to the degree of adjacent reentry. The have also not fully accounted for the effects of bending energy by not treating all three segment configurations on an equal statistical basis. This leads to an underestimate of the changes in the interphase due to chain stiffness.

Mansfield has investigated a variety of energetic effects on the chain configurations. For freely flexible chains, our results agree quite closely with his Monte Carlo results. He also finds a decrease in the number of 0th-layer tight folds and an increase in tight folds in subsequent layers as the bending energy increases. He predicts a more rapid change than found in the mean-field analysis presented here. For a bending energy $\epsilon_b = k_bT$, Mansfield found a decrease in the percentage of tight folds to 29% as compared to 52.2% found in this analysis.

References and Notes

(1) Flory, P. J. *J. Am. Chem. Soc.* **1962**, *84*, 2857.
(2) *Faraday Discuss Chem. Soc.* **1979**, 68.
(3) Peterlin, A. *Macromolecules* **1980**, *13*, 777.
(4) DiMarzio, E. A.; Guttman, C. M. *Polymer* **1980**, *13*, 733.
(5) Guttman, C. M.; DiMarzio, E. A.; Hoffman, J. D. *Polymer* **1981**, *22*, 1466.
(6) Guttman, C. M.; DiMarzio, E. A. *Macromolecules* **1982**, *15*, 525.
(7) Leermakers, F. A. M.; Scheutjens, J. M. H. M.; Gaylord, R. J. *Polymer* **1984**, *25*, 1577.
(8) Mansfield, M. G. *Macromolecules* **1983**, *16*, 914.
(9) Flory, P. J.; Yoon, D. Y.; Dill, K. A. *Macromolecules* **1984**, *17*, 862.
(10) Marqusee, J. A.; Dill, K. A. *Macromolecules* **1986**, *19*, 2420.
(11) Helfand, E. *J. Chem. Phys.* **1975**, *63*, 2192.
(12) Helfand, E. *Macromolecules* **1976**, *9*, 307.
(13) Weber, T. A.; Helfand, E. *Macromolecules* **1976**, *9*, 311.
(14) Yoon, D. Y.; Flory, P. J. *Macromolecules* **1984**, *17*, 868.